

Control of quarter electric vehicle based on PACEJKA tire model by fuzzy sliding controller

Rachida Baz¹, Khalid El Majdoub², Fouad Giri³, Ossama Ammari¹

¹Department of Electric Engineering, Faculty of Science and Technology, University Hassan II, Mohammedia, Morocco

²ENSEM, University Hassan II, Casablanca, Morocco

³Normandie University UNICAEN, Caen, France

Article Info

Article history:

Received Jun 23, 2024

Revised Dec 9, 2024

Accepted Dec 26, 2024

Keywords:

Fuzzy sliding mode

In-wheel BLDC motor

Longitudinal vehicle dynamic

PACEJKA tire model

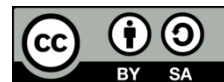
PI controller

Quarter electric vehicle

ABSTRACT

This paper presents the design of a hybrid intelligent fuzzy sliding controller (HIFSC) for a purely electric quarter vehicle (QEV) using a brushless DC (BLDC) motor and a PACEJKA tire model. The proposed system processes control signals to manage the QEV's dynamic longitudinal behavior. The BLDC motor and tire are modeled together to form an in-wheel motor system, which is inherently non-linear and subject to uncertainties. To address these challenges, an intelligent controller integrating sliding mode control (SMC) with fuzzy logic tuning is proposed. While SMC is effective in managing non-linearities, it is prone to chattering. The incorporation of fuzzy logic aims to mitigate this issue, ensuring stability and maintaining the sliding mode. The system and controller were simulated using MATLAB/Simulink. Simulation results demonstrate that the fuzzy sliding mode controller outperforms the conventional PI controller by reducing chattering and enhancing the system's sensitivity to external noise, without overshooting across various road conditions. Notably, the slip rate achieves a maximum of around 2.1% on wet roads.

This is an open access article under the [CC BY-SA](#) license.



Corresponding Author:

Rachida Baz

Department of Electric Engineering, Faculty of Science and Technology, University Hassan II
Mohammedia, Morocco

Email: rachida.baz@gmail.com

1. INTRODUCTION

Environmental protection challenges and the scarcity of energy resources have driven profound transformations in all scientific and industrial fields [1]. Advances in electronics and informatics have played a crucial role in this transformation [2]. This decade has seen rapid advancements in electric vehicles (EVs) [3], and commercial hybrid vehicles have swiftly entered the market [4]. Both academia and the automotive industry have focused extensively on the study of EV propulsion systems. They can be categorized based on their design, purpose, or energy source, and the electrification of traction systems is recognized as one of the most effective and modern solutions to reduce carbon emissions and fossil fuel usage [5]. This shift involves replacing internal combustion engines with electric motors, which convert electrical energy into mechanical energy to propel the vehicle.

In this study, the focus is on the brushless DC (BLDC) motor, which is directly coupled to the drive wheels to form an in-wheel motor incorporated into a purely electric vehicle, specifically a quarter electric vehicle (QEV) [6]-[8]. BLDC motors play a crucial role in electric drives across various industries, including automotive, industrial automation, robotics, and aviation [9]. These in-wheel BLDC motors provide enhanced vehicle stability and durability due to their independent controllability and quick, accurate response to commands [10]. The

interaction tire-road is governed by numerous parameters such as road surface characteristics and tire properties [11], with various models like the PACEJKA model [12], the Dugoff model [13], and the Kiencke model [14].

Precise control of electric motors is paramount in a wide range of industrial and commercial applications, from automation and robotics to transportation and power systems [15]. To meet the rigorous demands of these applications, motor control systems must offer high performance and robustness over a wide range of operating conditions [16]. Conventional linear controllers, such as proportional-integral (PI) and proportional-integral-derivative (PID) controllers, while relatively simple to design and implement, are often unable to effectively handle the complex, non-linear dynamics inherent in electric motor systems [17]. In response to these challenges, sliding mode control (SMC) has emerged as a promising alternative, attracting particular attention due to its inherent robustness to parameter variations and external disturbances [18], as well as its good tracking performance [19]. However, SMC is susceptible to the problem of “chattering”, a phenomenon that can degrade system performance and can be sensitive to noise. Consequently, intelligent and adaptive controllers have become increasingly important to overcome this issue [20]. This paper combines fuzzy logic for its advantages, such as the ability to handle non-linear systems, flexibility in rule-based decision-making, the ability to incorporate expert knowledge, and the ability to handle uncertainties [21], together with the SMC, it forms a hybrid intelligent fuzzy sliding mode controller (HIFSC) to regulate and control system speed. This approach improves the design and stability of the sliding surface, while HIFSC techniques provide a resilient control system with high disturbance rejection and transient performance [22]. It is modeled and analyzed on MATLAB software.

This article is structured as follows: i) Section 1 covers the modeling of the QEV, including vehicle dynamics, the BLDC motor in the wheel, and the PACEJKA tire model; ii) Section 2 designs the proposed fuzzy sliding controller; iii) Section 3 presents MATLAB/Simulink simulation results; iv) Section 4 describes the controller's performance; and v) Section 5 provides the conclusion.

2. METHOD

This part concerns the modeling of the studied system QEV, including the in-wheel BLDC motor, which offers the advantage of reducing vehicle space requirements, and the direct energy transfer from the motor to the wheel through a hybrid design consisting of active suspension and braking system, and taking into account the PACEJKA tire model.

2.1. Brushless DC motor modeling: mathematical aspects

An electric traction system employing a brushless DC motor (BLDC), shown in Figure 1(a), This motor is characterized by its ability to deliver performances similar to those of the brushed DC motor. On the other hand, the BLDC motor is based on electronic commutation instead of mechanical commutation [23]. Which is illustrated in Figure 1(b).

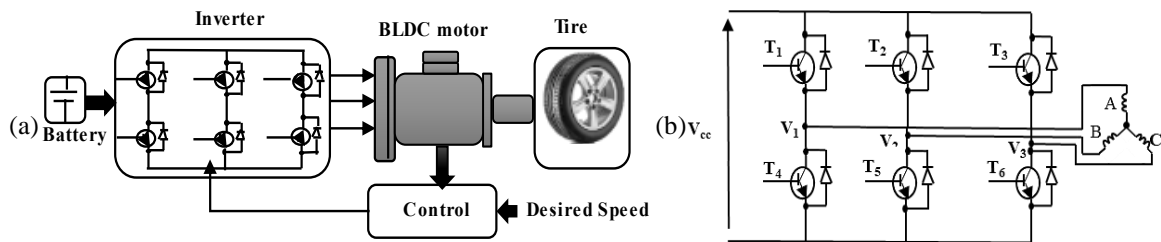


Figure 1. Schematic representation of an in-wheel motor traction system: (a) different components of electrical traction chain and (b) bridge driver circuit connected to BLDC motor

The following equations represent the voltage applied on the winding's motor for a balanced system with symmetrical windings and the back-EMF waveforms e_i are functions of rotor shaft angular velocity. Kirchhoff's voltage law is used to determine the results for the three-phase stator loop winding circuits.

$$V_a = R_a i_a + L_a \frac{di_a}{dt} + M_{ab} \frac{di_b}{dt} + M_{ac} \frac{di_c}{dt} + e_a \quad (1)$$

$$V_b = R_b i_b + L_b \frac{di_b}{dt} + M_{ba} \frac{di_a}{dt} + M_{bc} \frac{di_c}{dt} + e_b \quad (2)$$

$$V_c = R_c i_c + L_c \frac{di_c}{dt} + M_{ca} \frac{di_a}{dt} + M_{cb} \frac{di_b}{dt} + e_c \quad (3)$$

Where M_{ij} : interphase inductance (i-j), R_i : winding resistance by phase I, L_i : self-inductance by phase I, e_i : EMF by phase I, and V_i : voltage by phase i, where i or j refer to phases a, b, and c.

$$e = k_e \omega_m \quad (4)$$

Where k_e : is the back-emf constant.

The self-inductances are considered identical, especially if the motor is assumed to be surface-mounted, and all phase resistances are equal, in a balanced three-phase system. Therefore, the matrix equivalent of the following expression may be used to model the BLDC motor mathematically as (5).

$$\begin{bmatrix} L & M & M \\ M & L & M \\ M & M & L \end{bmatrix} \frac{d}{dt} \begin{bmatrix} i_a \\ i_b \\ i_c \end{bmatrix} = \begin{bmatrix} v_a \\ v_b \\ v_c \end{bmatrix} - \begin{bmatrix} R & 0 & 0 \\ 0 & R & 0 \\ 0 & 0 & R \end{bmatrix} \begin{bmatrix} i_a \\ i_b \\ i_c \end{bmatrix} - \begin{bmatrix} e_a \\ e_b \\ e_c \end{bmatrix} \quad (5)$$

The electromechanical torque is given by (6) and (7).

$$T_{em} = j_r \dot{\omega} + K_f \omega + T_L \quad (6)$$

$$T_{em} = \frac{1}{\omega_m (e_a i_a + e_b i_b + e_c i_c)} \quad (7)$$

2.2. Tire model

To Evaluate vehicle design more affordably than through physical testing. The interplay of tires and terrain is crucially relevant to the vehicle dynamics model, as it can significantly affect how a vehicle moves in a simulation [24]. In this paper, it is suggested that the tire be modeled using PACEJKA's tire model, known as the magic formula. The global equation of the tire model PACEJKA is illustrated as (8).

$$\mu(\sigma) = D \sin(C \tan^{-1}(B\sigma - E(B\sigma - \tan(B\sigma)))) \quad (8)$$

Where: B: the stiffness factor; D: the shape factor; C: the peak value; E: the curvature factor. The adhesion coefficient and the normal force F_v on the wheel are combined to obtain the longitudinal force F_x , as described in (9), also, the longitudinal slip is defined in (10).

$$\mu = \frac{F_x}{F_v} \quad (9)$$

$$\sigma = \frac{r\omega - v_x}{\max(v_x, r\omega)} \quad (10)$$

Where: r_{eff} : wheel radius (m); v_x : vehicle velocity (ms⁻¹); ω : wheel rotational velocity (rad/s).

2.3. Vehicle modelling

To determine the vehicle's acceleration and deceleration, by applying Newton's first law, which is founded on the equilibrium of the forces acting on the vehicle. Figure 2 describes the QEV longitudinal model, considering that the impacts of lateral and vertical forces are neglected, the movement followed is linear.

$$m\dot{v}_x = F_x \quad (11)$$

Where: m : the masse of the quarter vehicle (kg), \dot{v}_x : the velocity of the vehicle (m/s), F_x : the traction force generated between the tire and the road surface acting on the wheel (N).

Applying Newton's second law, which specifies that the product of the inertia tensor J and the rotational acceleration along the axis under consideration, taking into account rolling resistance, yields as (12).

$$T_e = J\dot{\Omega}_\omega + F_x r_{eff} + M_{rr} \quad (12)$$

Where T_e : the electromagnetic torque produced by the in-wheel motor (Nm), J : the moment of inertia of the driving wheel (kgm²), $\dot{\Omega}_\omega$: the rotational velocity of the driving wheel (rads-1), F_x : is the traction or braking force (N), and M_{rr} : rolling resistance.

The force responsible for movement from the central point to a distance $d_{rr, \max}$, which is referred to as the maximal trail of vertical load, produces a compensatory torque M_{rr} that is known as rolling resistance [25], which is represented in the (13), Where μ_{rr} is the rolling resistance factor and F_v the normal force.

$$M_{rr} = F_v \mu_{rr} r_{eff} \quad (13)$$

The performance of the driver immediately affects the vehicle's safety and efficiency and plays a significant part in how the vehicle is controlled. the speed control model deployed in this work is a filtered control to assimilate the driver's behavior of the vehicle during either acceleration or deceleration, as represented in Figure 3.

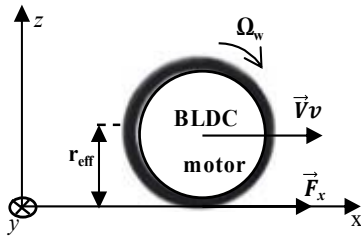


Figure 2. Quarter vehicle longitudinal model

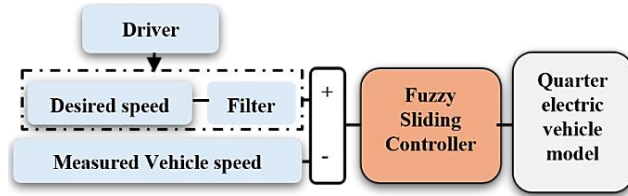


Figure 3. Schematic diagram of the driver model

2.4. Design of the controller based on sliding mode and fuzzy logic

The sliding mode controller (SMC) is a variable structure controller (VSC) [26]. It utilizes different continuous functions to relate the system state to a command. The system's state is represented by a switching function, which determines the appropriate function to use. In this context, U represents the control input.

$$U = -Ksgn\left(\frac{S}{\phi}\right) \quad (14)$$

Where, the constant factor ϕ is the thickness of the boundary layer, and S is the sliding surface.

In order to attain the sliding surface in a finite time, a positive constant has been chosen. The issue in this control mode is chatter if a sign function is used [27]. To remedy this, a saturation function is used to bind the sliding surface as shown in (15), which is defined in (16) [28]. The aim of developing a sliding-mode controller for plants of all orders is to reduce the derivative and error of these variables to zero. If the sliding mode is active, the switching surface regulates the system's transient responsiveness [29]. The structure of the switching surface includes the construction of the switching behavior.

$$U = -Ksat\left(\frac{S}{\phi}\right) \quad (15)$$

$$sat\left(\frac{S}{\phi}\right) = \begin{cases} \frac{S}{\phi}, & |S/\phi| \leq 1 \\ sgn\left(\frac{S}{\phi}\right), & |S/\phi| > 1 \end{cases} \quad (16)$$

The control law allows a trajectory to lean towards the sliding surface $S=0$ and maintain it regardless of the initial condition, provided the condition below is met.

$$S\dot{S} \leq -\eta|S| \quad (17)$$

The error of a variable is initiated at zero, and this is where the localization error initially appears.

$$e = V_{ref} - V \quad (18)$$

$$S = \dot{e} + \lambda_1 e + \lambda_2 \int e dt \quad (19)$$

Were $\lambda_1, \lambda_2 > 0$ as strictly real constants.

The sliding mode is characterized by non-linear properties and the problem of chattering, which is mainly caused by the K gain. In order to reduce the chattering effect and improve system performance, a hybrid controller has been proposed that integrates two control modes, SMC and fuzzy, to adjust the K_{fuzzy} gain value according to time. The theory of fuzzy set, originally developed by Zadeh in 1965, is the foundation of fuzzy logic [30]. The black box contains a technique to integrate the input data into the output through accurate information. The input and output mapping are shown in Figure 4 as payload data.

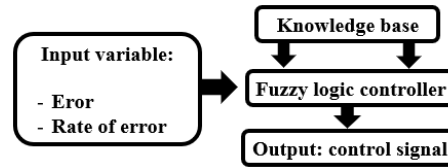


Figure 4. Input-output mapping and knowledge base

3. RESULT AND DISCUSSION

The inputs of the fuzzy corrector are S and \dot{S} , the output is K_{Fuzzy} . The fact that $S\dot{S} < 0$ is a prerequisite for the development of a sliding mode surface. The switch gain $K_{Fuzzy}(t)$ value ought to always ensure the fulfillment of the aforementioned criterion. As a result, the controller will use the value of S and \dot{S} as its input. The output, the switching gain, is denoted by the symbol K_{Fuzzy} . Each linguistic variable of a fuzzy set has its membership functions illustrated in Figure 5. The fuzzy control rules are shown in Table 1. The variables' fuzzy sets are defined by: $\dot{S} = \{Nb, Ns, Z, Ps, PB\}$; $S = \{N, Z, P\}$; $K_{Fuzzy} = \{S, M, B\}$.

The model parameters for the understudied quarter vehicle are shown in Table 2 of this study. The model was developed using MATLAB/Simulink. The efficiency of the controller will be assessed during acceleration and deceleration on various types of roadways (dry and wet), and then it will be compared with the system response controlled by the PI controller.

The simulation was carried out as shown in Figure 6, assuming that the vehicle was already on the road at a speed of 60 Km/h, and taking the steps shown in Table 3. The white noise represents 5% of the desired speed applied by the driver. The driver's command is represented in Figure 7. The response of the system studied under the PI controller and HIFSMC is shown in Table 3.

Table 1. The rule base of K_{Fuzzy}

S	\dot{S}				
	Nb	Ns	Z	Ps	PB
N	B	M	M	S	B
Z	B	M	S	M	B
P	B	S	M	B	B

Table 2. Parameters for the studied system and the BLDC motor

Symbol	Description	Value
g	Gravity acceleration	9.81 m s ⁻²
J	Moment of inertia of the driving wheel	0.75 kg.m ²
M	Mass of quarter of the vehicle	270 kg
r_{eff}	Wheel radius	0.32 m
μ_{rr}	Coefficient of rolling resistance	0.025
Motor parameter		
L	Inductance	8.5e-4 H
j_r	Rotor inertia	1 kg.m ²
R	Stator resistance	0.2 Ω

Table 3. Simulation conditions on dry and wet road during acceleration and deceleration

Time interval (Sec)	Speed (Km/h)	Road type	Noise
0-5	80	Dry	0%
5-10	60	Dry	0%
10-15	80	Wet	0%
15-20	80	Dry	0%
20-25	80	Dry	5%

Figure 8 shows the vehicle and wheel speed in reference to the setpoint given by the driver during acceleration and deceleration controlled by the PI controller. The wheel speed tracks the setpoint, but the vehicle speed shows a significant delay, influencing wheel slip. Secondly, the disturbances applied to the system at 20 sec are not attenuated but seriously affect the wheel speed, which reaches 82.9 Km/h, exceeding the 80 Km/h setpoint.

The vehicle and the wheel speed, and response of the HIFSMC controller, are shown in Figure 9, they follow the filtered command of the driver in the different stages: acceleration and deceleration. Furthermore,

this model shows good resistance to disturbance applied to the system after 20 sec. According to the simulation of the two controllers, the slip ratio of the system controlled by PI reaches a maximum value of 11% on a dry road but has no noise resistance, which can negatively affect the wheel's condition while driving, and a minimum value of 3.5%, as depicted in Figure 10(a). The HIFSMC performs better in terms of noise resistance than the conventional PI controller, so the slip ratio parameter is improved, with 1.9% during acceleration on a dry asphalt road and 2.1% on a wet road, and it has a negative value during deceleration which is -1.5%, in addition, it has a significant response against white noise, as illustrated in Figure 10(b). The longitudinal force F_x changes from 1800 N during the acceleration phase to -1500 N during the deceleration phase, as shown in Figure 11.

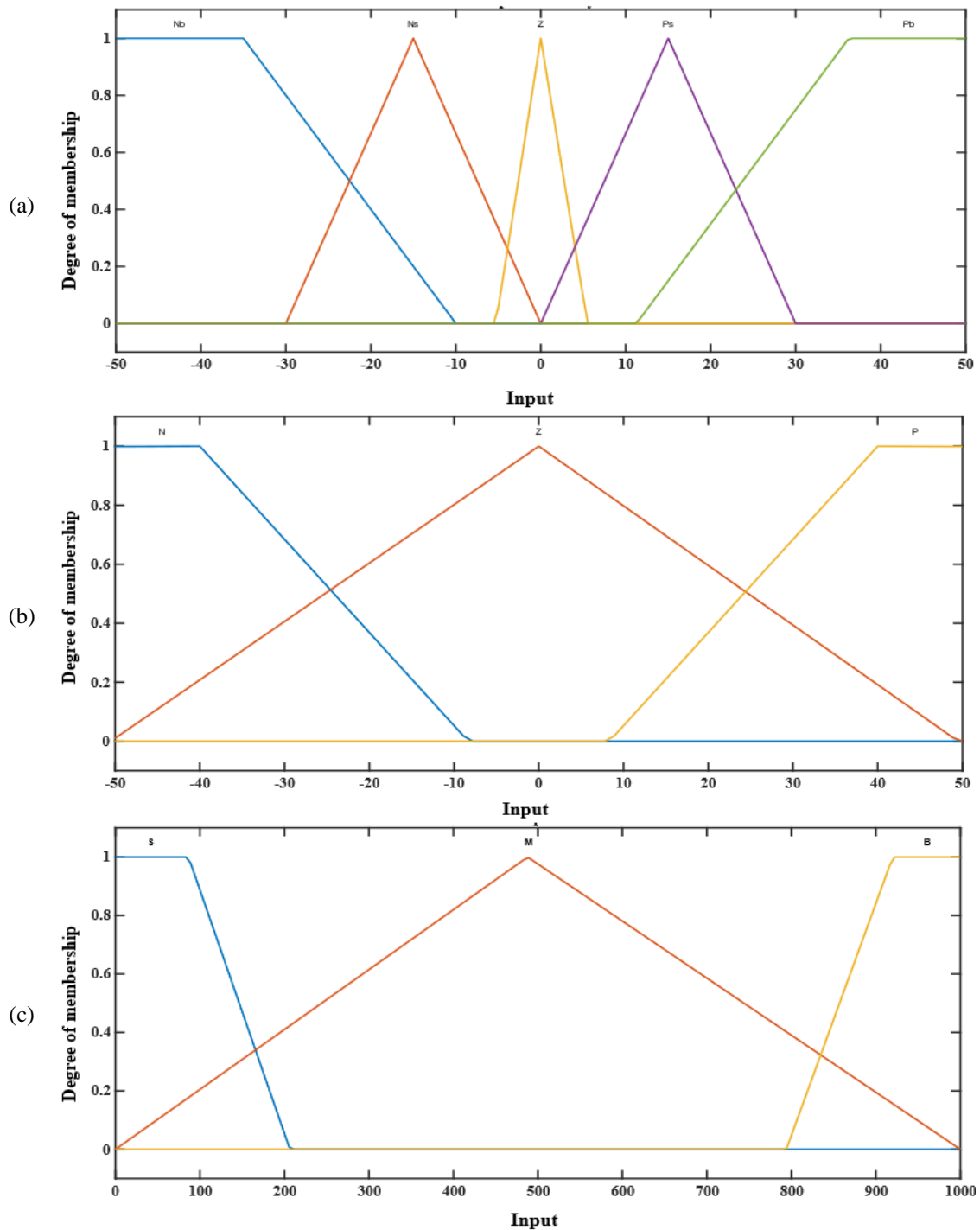


Figure 5. Membership functions for (a) input variable ' \dot{S} ', (b) input variable ' S ', and (c) input variable ' K_{Fuzzy} '

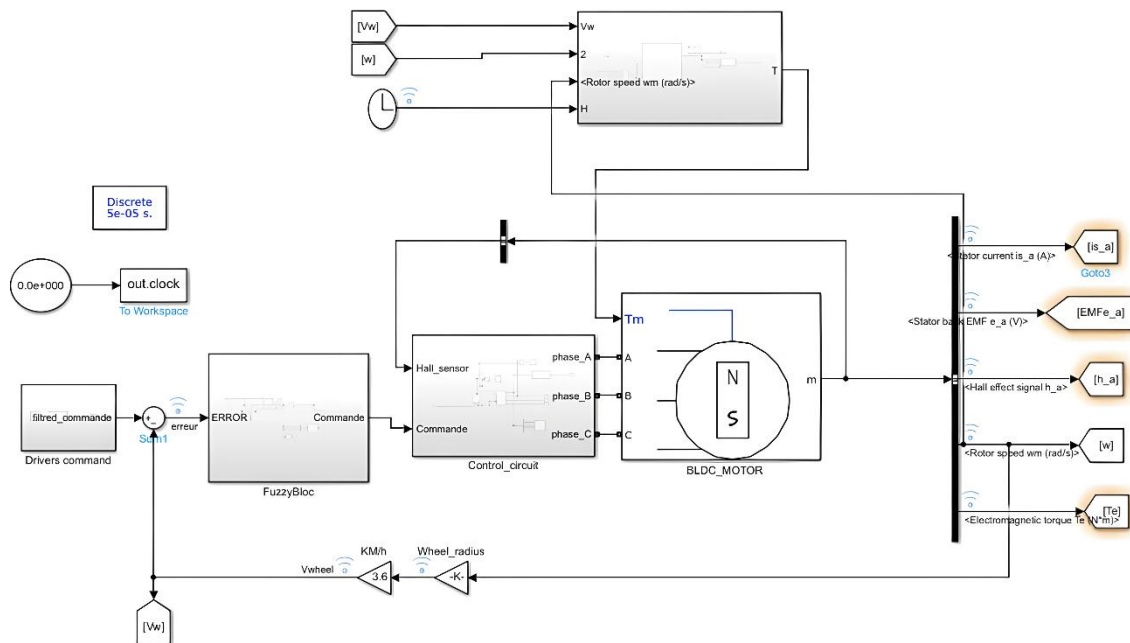


Figure 6. System dynamic model in Simulink associated to the in-wheel-motor

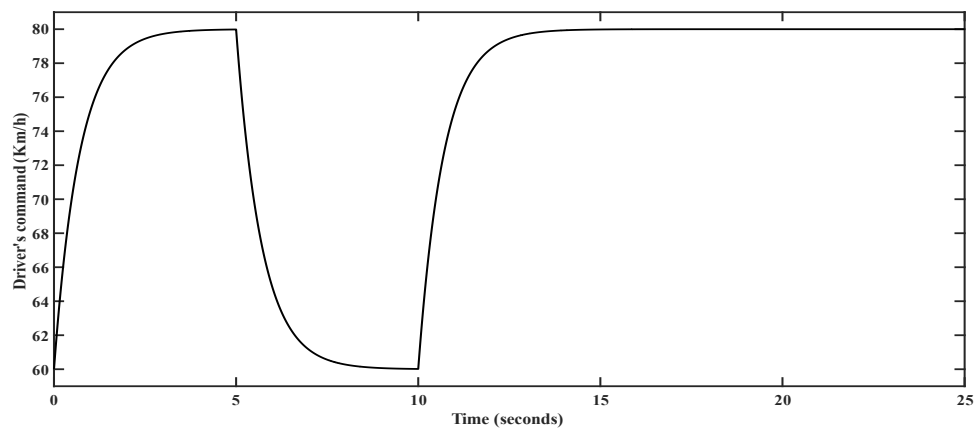


Figure 7. The driver's command in different stages of driving

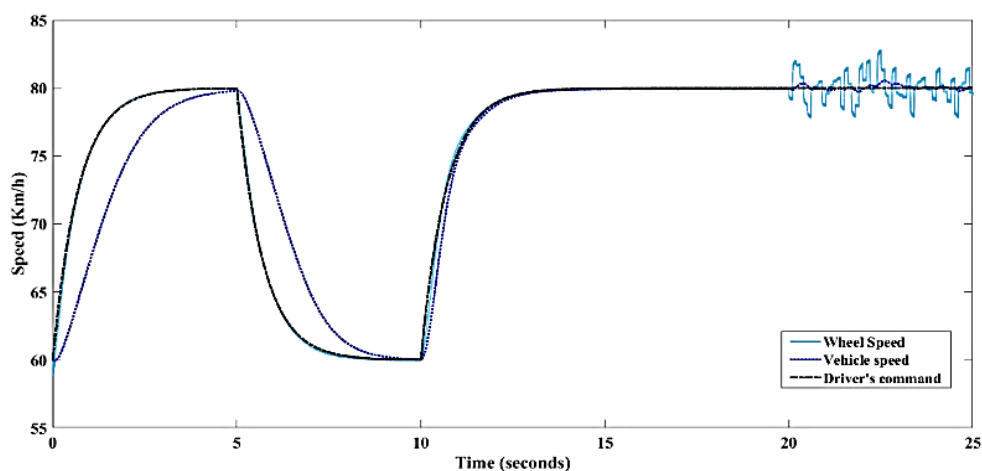


Figure 8. Speed system's response controlled by PI controller (Km/h) in dry and wet road

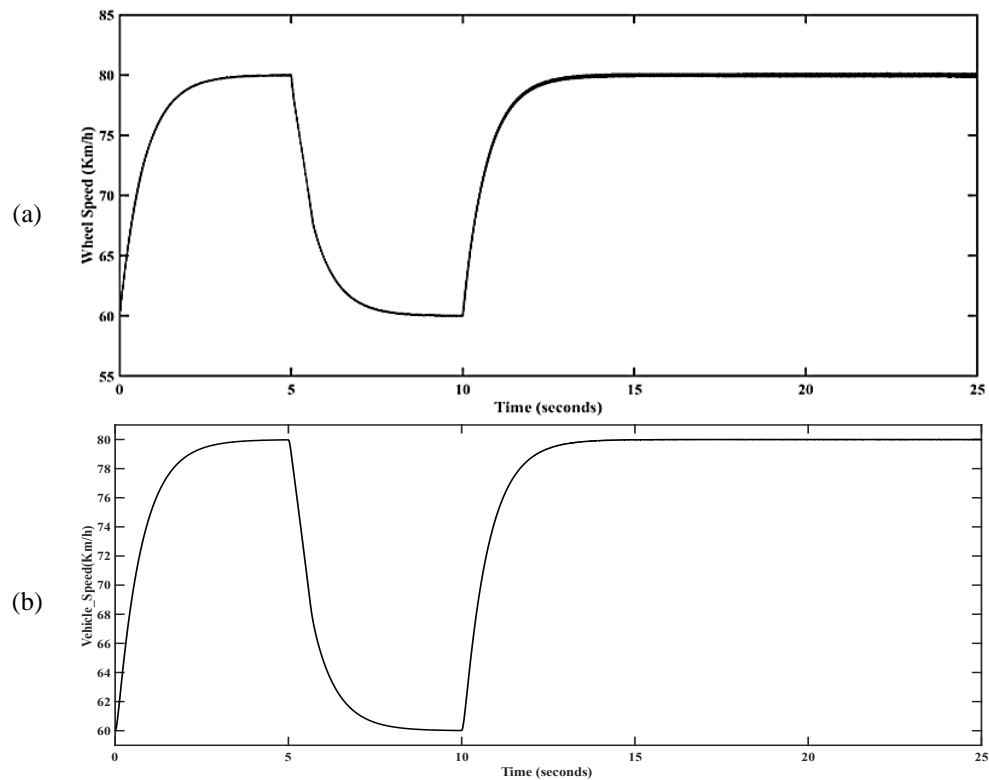


Figure 9. System response of the HIFSM controller: (a) response of wheel speed V_w [Km/h] and (b) response of vehicle speed V_v [Km/h]

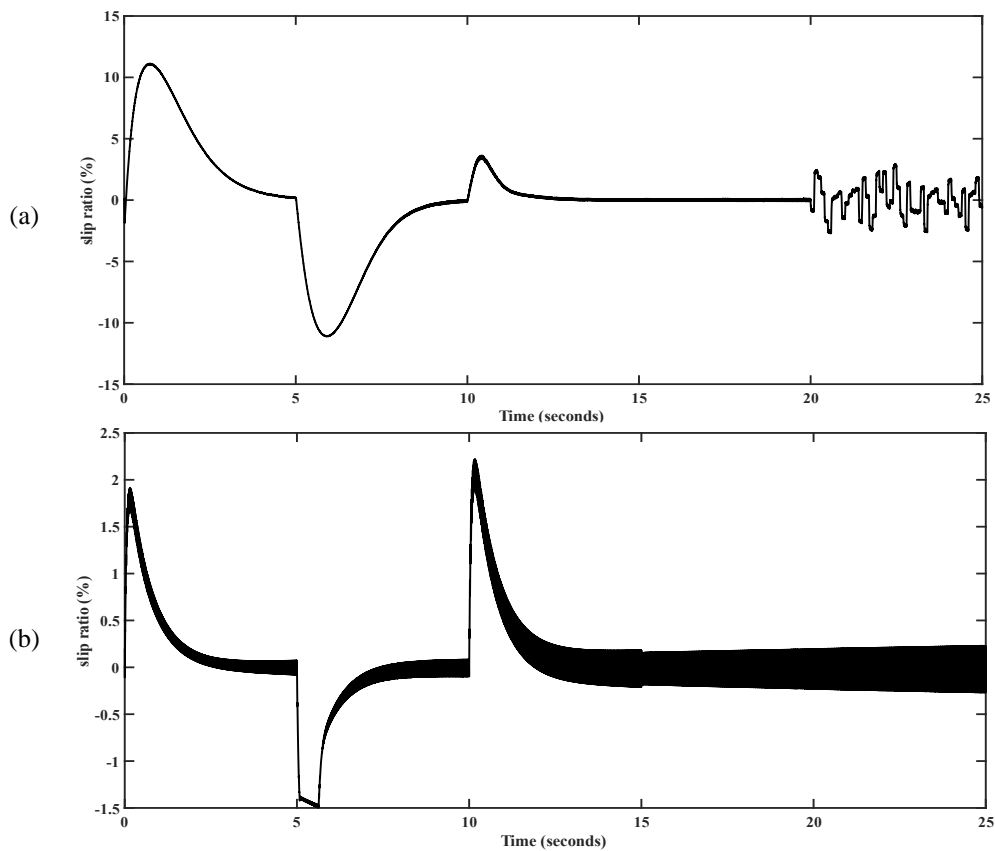


Figure 10. Slip ratio generated by the QEV: (a) controlled by PI controller and (b) controlled by HIFSMC

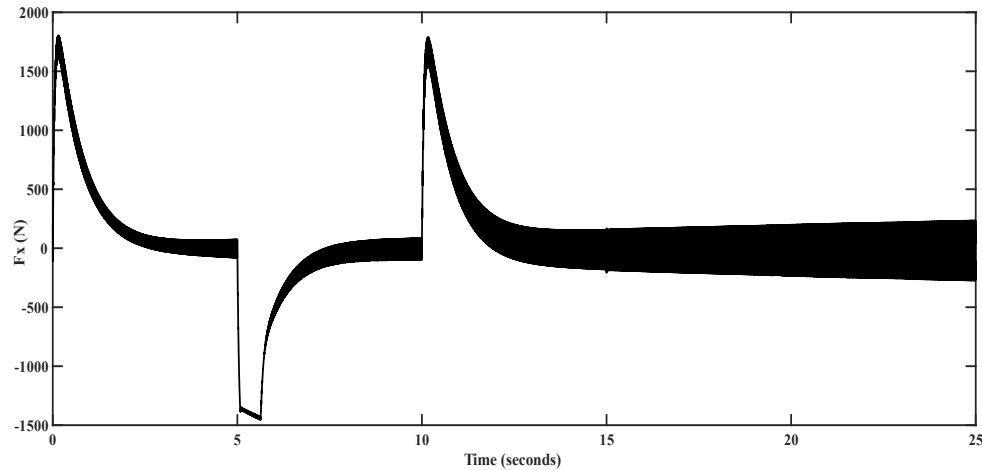


Figure 11. Measured longitudinal force $F_x(N)$ during driving conditions

Table 4 depicts a comparison between the method adopted in this work and recent studies. The study [31] presents an improvement in the dynamic performance of a semi-active suspension system coupled to an active aerodynamic surface but at the expense of a compromise between comfort and grip, which limits its adaptability to varied real-world conditions. The work [32] offers the advantage of stable speed control, ensuring smooth system response thanks to a fuzzy PID controller; however, its noise resistance remains inferior to that of current work. The study [33] highlights a detailed comparison of direct torque control (DTC), fuzzy direct torque control (FDTC), and model predictive direct torque control (MPDTC) techniques for reducing torque and flux ripples in a PMSM motor. Nevertheless, the MPDTC approach presents notable complexity, posing a challenge to its industrial adoption.

On the other hand, the proposed work, based on an intelligent hybrid fuzzy and sliding mode controller (HFSMC), demonstrates remarkable robustness and resistance to external disturbances compared with other studies, even under difficult driving conditions (dry and wet roads, during acceleration and deceleration phases). With a slip rate reduced to 2.1%, it guarantees enhanced safety and comfort. However, it suffers from considerable design complexity, a disadvantage that can be offset by its robustness in a various demanding environment.

Table 4. Comparative analysis of the proposed method with recent studies

Study	Methodology	Controller	Advantages	Limitations
Abbas <i>et al.</i> [31]	Optimum control of a semi-active suspension with active aerodynamic surface (AAS).	LQR controller to optimize dynamic performance.	- Reduced vibration and improved adhesion	- Need for a compromise between comfort and adhesion.
Baz <i>et al.</i> [32]	Speed control of an electric vehicle with a BLDC motor integrated into the wheel.	Fuzzy PID control with electromechanical modeling	- Stable and smooth speed control.	- Important number of fuzzy rules (49×3 parameters). - Low noise resistance.
Kakouche <i>et al.</i> , [33]	Simulation in MATLAB/Simulink with NYCC to evaluate ripples for PMSM in EVs.	DTC, FDTC and MPDTC for PMSM in EV.	- Significant reduction in torque, flux, and speed ripples.	- Complex numerical implementation for MPDTC.
The proposed work	Longitudinal control with HFSMC of a QEV with PACEJKA tire model and integrated BLDC.	HFSMC to resolve non-linearities.	- Stable speed regulation - Adaptability to road variations. - High resistance to disturbance and reduced chattering noise.	- Chattering phenomena on the conventional SMC

4. CONCLUSION

The proposed hybrid control strategy, based on a fuzzy sliding mode, has proven highly effective in regulating the speed of an electric vehicle equipped with a BLDC motor integrated into the wheel. The model incorporates the PACEJKA tire model and employs a filtered control system to represent the driver. Implemented in MATLAB/Simulink, the speed controller utilizes a fuzzy sliding mode control strategy. To mitigate noise within the control system, the fuzzy theory is applied to adjust the K_{fuzzy} parameter. The results demonstrate exceptional setpoint tracking accuracy, maintaining high steering speed precision on dry and wet roads. Moreover, the system exhibits robust performance, remaining unaffected by external disturbances. The hybrid control strategy ensures superior dynamic characteristics compared to the conventional PI controller, validating the effectiveness of the HFSMC, particularly in improving the slip ratio. Future research could

delve into optimizing controller parameters for diverse driving conditions and exploring hybridization with other methods to circumvent the challenges of designing suitable fuzzy rules. These advancements would further enhance the performance and driving comfort of electric vehicles.





REFERENCES

- [1] Y. Luo *et al.*, "Development and application of fuel cells in the automobile industry," *Journal of Energy Storage*, vol. 42, p. 103124, Oct. 2021, doi: 10.1016/j.est.2021.103124.
- [2] M. S. Sarfraz, H. Hong, and S. S. Kim, "Recent developments in the manufacturing technologies of composite components and their cost-effectiveness in the automotive industry: A review study," *Composite Structures*, vol. 266, 2021, doi: 10.1016/j.compstruct.2021.113864.
- [3] A. Mahdavian, A. Shojaei, S. McCormick, T. Papandreou, N. Eluru, and A. A. Oloufa, "Drivers and barriers to implementation of connected, automated, shared, and electric vehicles: An agenda for future research," *IEEE Access*, vol. 9, pp. 22195–22213, 2021, doi: 10.1109/ACCESS.2021.3056025.
- [4] F. Zhang, L. Wang, S. Coskun, H. Pang, Y. Cui, and J. Xi, "Energy management strategies for hybrid electric vehicles: Review, classification, comparison, and outlook," *Energies (Basel)*, vol. 13, no. 13, p. 3352, Jun. 2020, doi: 10.3390/en13133352.
- [5] C. Guo, L. Long, Y. Wu, K. Xu, and H. Ye, "Electromagnetic-thermal coupling analysis of a permanent-magnet in-wheel motor with cooling channels in the deepened stator slots," *Case Studies in Thermal Engineering*, vol. 35, 2022, doi: 10.1016/j.csite.2022.102158.
- [6] A. Karki, S. Phuyal, D. Tuladhar, S. Basnet, and B. Shrestha, "Status of pure electric vehicle power train technology and future prospects," *Applied System Innovation*, vol. 3, no. 3, p. 35, Aug. 2020, doi: 10.3390/asi3030035.
- [7] A. Shaju and A. K. Pandey, "Modelling transient response using PAC 2002-based tyre model," *Vehicle System Dynamics*, vol. 60, no. 1, pp. 20–46, Jan. 2022, doi: 10.1080/00423114.2020.1802048.
- [8] O. Ammari, K. EL Majdoub, F. Giri, and R. Baz, "Modeling and control design for half electric vehicle with wheel BLDC actuator and PACEJKA's tire," *Computers and Electrical Engineering*, vol. 116, May 2024, doi: 10.1016/j.compeleceng.2024.109163.
- [9] D. Mohanraj *et al.*, "A review of BLDC motor: State of art, advanced control techniques, and applications," *IEEE Access*, vol. 10, pp. 54833–54869, 2022, doi: 10.1109/ACCESS.2022.3175011.
- [10] A. S. Cabuk, "Effect of ferromagnetic materials on vibration of in-wheel brushless direct current motor for light electric vehicle," *Journal of Electrical Engineering & Technology*, Aug. 2024, doi: 10.1007/s42835-024-02029-w.
- [11] V. F. Vázquez *et al.*, "Tire/road noise, texture, and vertical accelerations: Surface assessment of an urban road," *Applied Acoustics*, vol. 160, p. 107153, Mar. 2020, doi: 10.1016/j.apacoust.2019.107153.
- [12] A. Ružinskas and H. Sivilevičius, "Magic formula tyre model application for a tyre-ice interaction," *Procedia Engineering*, vol. 187, pp. 335–341, 2017, doi: 10.1016/j.proeng.2017.04.383.
- [13] S. Savant, H. D. C. Pinheiro, M. E. Sacchi, C. Conti, and M. Carello, "Tires and vehicle lateral dynamic performance: A corrective algorithm for the influence of temperature," *Machines*, vol. 11, no. 6, p. 654, Jun. 2023, doi: 10.3390/machines11060654.
- [14] H. B. Moussa and M. Bakhti, "Extended Kalman filter based lateral velocity and yaw rate estimation for a vehicle with nonlinear tire model," in *Lecture Notes in Electrical Engineering*, vol. 1141 LNEE, 2024, pp. 618–629, doi: 10.1007/978-981-97-0126-1_55.
- [15] M. Soori, B. Arezoo, and R. Dastres, "Optimization of energy consumption in industrial robots, a review," *Cognitive Robotics*, vol. 3, pp. 142–157, 2023, doi: 10.1016/j.cogr.2023.05.003.
- [16] M. Gobbi, A. Sattar, R. Palazzetti, and G. Mastinu, "Traction motors for electric vehicles: Maximization of mechanical efficiency – A review," *Applied Energy*, vol. 357, p. 122496, Mar. 2024, doi: 10.1016/j.apenergy.2023.122496.
- [17] L. Quan and W. Zhao, "A review on positioning uncertainty in motion control for machine tool feed drives," *Precision Engineering*, vol. 88, pp. 428–448, Jun. 2024, doi: 10.1016/j.precisioneng.2024.03.003.
- [18] S. J. Gambhire, D. R. Kishore, P. S. Londhe, and S. N. Pawar, "Review of sliding mode based control techniques for control system applications," *International Journal of Dynamics and Control*, vol. 9, no. 1, pp. 363–378, 2021, doi: 10.1007/s40435-020-00638-7.
- [19] Y. Wang, Z. Zhang, C. Li, and M. Buss, "Adaptive incremental sliding mode control for a robot manipulator," *Mechatronics*, vol. 82, p. 102717, Apr. 2022, doi: 10.1016/j.mechatronics.2021.102717.
- [20] S. M. Amr and A. Alturki, "Robust control design for an active magnetic bearing system using advanced adaptive SMC technique," *IEEE Access*, vol. 9, pp. 155662–155672, 2021, doi: 10.1109/ACCESS.2021.3129140.
- [21] M. Alateeq and W. Pedrycz, "Logic-oriented fuzzy neural networks: A survey," *Expert Systems with Applications*, vol. 257, p. 125120, Dec. 2024, doi: 10.1016/j.eswa.2024.125120.
- [22] A. P. K.M. and U. Nair, "Intelligent fuzzy sliding mode controller based on FPGA for the speed control of a BLDC motor," *International Journal of Power Electronics and Drive Systems (IJPEDS)*, vol. 11, no. 1, pp. 477–486, Mar. 2020, doi: 10.11591/ijpeds.v11.i1.pp477-486.
- [23] M. P. Thakre and N. Kumar, "Design, development, and simulation modeling of hybrid electric vehicles incorporating with BLDC drive," in *Energy Systems in Electrical Engineering*, vol. Part F2138, 2022, pp. 513–551, doi: 10.1007/978-981-19-0979-5_20.
- [24] S. Boyle, "PACEJKA magic formula tire model parser," in *2019 International Conference on Computational Science and Computational Intelligence (CSCI)*, IEEE, Dec. 2019, pp. 517–518, doi: 10.1109/CSCI49370.2019.00099.
- [25] R. Baz, K. El Majdoub, F. Giri, and O. Ammari, "Modeling and adaptive neuro-fuzzy inference system control of quarter electric vehicle," *Indonesian Journal of Electrical Engineering and Computer Science*, vol. 34, no. 2, p. 745, May 2024, doi: 10.11591/ijeecs.v34.i2.pp745-755.
- [26] R. Rahmatullah, A. Ak, and N. F. O. Serteller, "Design of sliding mode control using SVPWM modulation method for speed control of induction motor," *Transportation Research Procedia*, vol. 70, pp. 226–233, 2023, doi: 10.1016/j.trpro.2023.11.023.
- [27] K. Makhoulfi, I. K. Bousserhane, and S. A. Zegnoun, "Adaptive fuzzy sliding mode controller design for PMLSM position control," *International Journal of Power Electronics and Drive Systems (IJPEDS)*, vol. 12, no. 2, p. 674, Jun. 2021, doi: 10.11591/ijpeds.v12.i2.pp674-684.
- [28] G. Tarchała and T. Orłowska-Kowalska, "Discrete sliding mode speed control of induction motor using time-varying switching line," *Electronics (Basel)*, vol. 9, no. 1, p. 185, Jan. 2020, doi: 10.3390/electronics9010185.
- [29] J. George and G. Mani, "A portrayal of sliding mode control through adaptive neuro fuzzy inference system with optimization perspective," *IEEE Access*, vol. 12, pp. 3222–3239, 2024, doi: 10.1109/ACCESS.2023.3348836.
- [30] B. Xiao, H.-K. Lam, K. Tanaka, and J. M. Mendel, "Guest editorial: Special issue on type-2 fuzzy-model-based control and its applications," *IEEE Transactions on Fuzzy Systems*, vol. 29, no. 2, pp. 199–202, Feb. 2021, doi: 10.1109/TFUZZ.2020.3046933.
- [31] S. B. Abbas and I. Youn, "Optimal control of a semi-active suspension system collaborated by an active aerodynamic surface based on a quarter-car model," *Electronics (Basel)*, vol. 13, no. 19, p. 3884, Sep. 2024, doi: 10.3390/electronics13193884.





- [32] R. Baz, K. El Majdoub, F. Giri, and A. Taouni, "Self-tuning fuzzy PID speed controller for quarter electric vehicle driven by in-wheel BLDC motor and PACEJKA's tire model," *IFAC-PapersOnLine*, vol. 55, no. 12, 2022, doi: 10.1016/j.ifacol.2022.07.377.
- [33] K. Kakouche, A. Oubelaid, S. Mezani, D. Rekioua, and T. Rekioua, "Different control techniques of permanent magnet synchronous motor with fuzzy logic for electric vehicles: analysis, modelling, and comparison," *Energies (Basel)*, vol. 16, no. 7, p. 3116, Mar. 2023, doi: 10.3390/en16073116.

BIOGRAPHIES OF AUTHORS







Rachida Baz     got in 2014 her License degree in Informatic and Electronics, at the Faculty of Science and Technology Mohammedia affiliated with the University Hassan II at Casablanca-Morocco, then she got a master's degree in biomedical engineering from the Faculty of Science and Technology, Settat, Morocco in 2019. She is currently a Ph.D. student in the Laboratory of Matter, Energy, and System Control (LMECS) at Hassan II University, Mohammedia-Casablanca, Morocco. Her works, studies, and interests focused on modeling, observation, electric, and hybrid vehicle control. She can be contacted at email: rachida.baz@gmail.com.







Khalid El Majdoub     received a Ph.D. degree in automatic control from the Mohammadia School of Engineering in Rabat (Morocco) in 2012. In 2001, he was an Aggregated Professor (Professeur Agrégé) in electrical engineering from the Ecole Normale Supérieure of Rabat, Morocco. Currently, he is serving as a Professor in the Engineering School of Electricity and Mechanic ENSEM affiliated to the University Hassan II at Casablanca-Morocco, where he teaches electrical engineering. His main research areas are nonlinear system control and observation, adaptive control, electric vehicle, hybrid electric vehicle control, and magnetorheological suspension control. He can be contacted at email: khalid_majdoub@yahoo.fr.



Fouad Giri     received the Ph.D. degree in automatic control from the Institute National Polytechnique de Grenoble, France, in 1988. He is currently a Professor at the University de Caen Normandie, France. His research interests include nonlinear system identification, observation, and control for finite- and infinite-dimensional systems and application to power electric systems. He has published 6 books and over 120 journal papers. He has served as a chair of the IFAC TC1.2 and associate editor for several journals including automatic, control engineering practice, IEEE Transactions on control systems technology. He can be contacted at email: fouad.giri@unicaen.fr.



Ossama Ammari     was born in 1990 in Casablanca, Morocco. In 2016, he was an aggregated professor (Professeur Agrégé) in electrical engineering from the Centre Régional des Métiers de l'Éducation et de la Formation Casablanca-Settat, Morocco. He received a master's degree in electrical engineering from the Faculty of Science and Technology, University Cadi Ayyad, Marrakech, Morocco, in 2013. The main research areas are nonlinear system control, adaptive control, electric vehicle, and hybrid electric vehicle control. He can be contacted at email: ammari.ossama@gmail.com.